

Spatiotemporal Variation of Interception in an Agriculture Watershed—Tadepalligudem, West Godavari, India



Rajkumar Tammiseti, Reshma Talari, and Savitha Chirasmayee

Abstract Interception refers to the quantity of rainfall prevented by vegetation from reaching the soil surface, which is one of the significant and integral parts of the hydrological cycle. Most hydrological models depend on the water balance components, where the rainfall intercepted by vegetation is considered a loss. It is an essential and controlling parameter in hydrological modeling studies and flood forecasting analysis, thus establishing that its impacts at local, regional, and global scales are imminent. Remote sensing is one of the advanced techniques that helps generate a spatiotemporal variation of interception by vegetation canopy. The present study aimed to generate spatiotemporal variation interception maps for an agricultural watershed covering 53.75 km² of the area near Tadepalligudem, West Godavari district, Andhra Pradesh. The study area is covered with vegetation cover that constitutes about 40–55% of the total catchment; thus, interception is a critical component in hydrological modeling studies in this watershed. Landsat 8 datasets acquired from USGS EarthExplorer during different months of 2020 are used in this study. Leaf area index (LAI) and canopy storage capacity (S_{\max}) are the influential parameters in estimating canopy rainfall interception. The interception maps at varying spatial and temporal scales are generated using MATLAB programming platform. The result obtained gives a better understanding of the spatiotemporal variation of interception and its importance at a regional scale. The canopy rainfall interception model derived can be applied to various agriculture watersheds. Further, results obtained from the analysis can be used in rainfall–runoff modeling and water resource management studies.

Keywords Interception · Remote sensing · Leaf area index · Canopy storage capacity

R. Tammiseti (✉) · R. Talari · S. Chirasmayee
Department of Civil Engineering, National Institute of Technology, Tadepalligudem, Andhra Pradesh 543101, India
e-mail: rajkumar.sclr@nitandhra.ac.in

R. Talari
e-mail: reshma@nitandhra.ac.in

© The Author(s), under exclusive license to Springer Nature Singapore Pte Ltd. 2023
P. V. Timbadiya et al. (eds.), *Hydrology and Hydrologic Modelling*,
Lecture Notes in Civil Engineering 312,
https://doi.org/10.1007/978-981-19-9147-9_33

409

1 Introduction

Interception is one of the critical parameters of the hydrological process, which indicates the amount of precipitation lost due to vegetation interception. Interception is a crucial process because it influences other hydrological processes like an infiltration, evapotranspiration, runoff generation, and flood generation [1, 2]. Considering interception by vegetation as an essential parameter of the hydrological processes in the water balance cycle helps achieve accurate runoff estimation analysis [3]. Interception also plays a vital role in water resource management and climate change. The appraisal of vegetation canopy interception is remarkably significant for describing and interpreting water cycling and has possible suggestions for land use–land cover planning and water and soil conservation [4].

The interception by vegetation cannot be determined directly. Interception is usually estimated as the difference between total rainfall and the sum of stem flow and through fall [5, 6] which is generally determined by studying an individual plant or group of plantations. Although collecting data from individual plants or groups of plantations gives high estimation accuracy, it is an expensive and time-consuming process and also interpolating it to a large study area becomes a difficult task. Modeling provides an excellent solution to generate a spatiotemporal variation of interception to a large study area in a short time [7, 8]. Canopy storage capacity (S_{\max}) is one of the critical parameters mentioned in best existing models like the Rutter model [9, 10] and Gash model [11], which indicated that excess rainfall would most likely result in water overflow through the canopy and toward the canopy ground surface [3, 5]. So, canopy storage capacity controls the rainfall interception by vegetation cover [12–14]. Studies showed that canopy storage capacity could be derived using leaf area index (LAI), which is generated using remote sensing data [15, 16]. Remote sensing is emerging as an effective tool for studying spatial and temporal variations of the land surface, which covers a wide range of vegetation indices used in this study. The study area (Tadepalligudem region) falls tropical part of India and is also close to Godavari delta regions with very fertile soil. The study area is covered a quality amount of vegetation throughout the year, so rainfall interception by the canopy plays a significant part in runoff analysis.

Most studies have been focused on estimating interception using a Geographic Information System (ArcGIS), which requires you to give the numerical equations as input in using a Raster Calculator tool each time to perform the analysis. The present study is aimed to develop a canopy rainfall interception model using a programming language for the estimation of rainfall loss due to vegetation in the form of interception. Landsat 8 satellite data with 30 m resolution is used as an input in the model. Maps are generated for different periods in 2019, 2020 and 2021, using the canopy rainfall interception model for three different precipitation scenarios. This model gives a better understanding of the relation between canopy storage capacity (S_{\max}), canopy rainfall interception (S_v), and precipitation. This estimated interception by vegetation could be further used in assessing the water balance cycle and hydrological analysis within this study region.

2 Materials and Methods

2.1 Study Area

The study area falls between $81^{\circ} 28'$ and $81^{\circ} 32' 30''$ east longitude and $16^{\circ}48' 30''$ and $16^{\circ} 54' 30''$ north latitude. Figure 1 shows the location of the study area in the Tadepalligudem region of West Godavari district (Andhra Pradesh). The total area covered under the study region is about 53.75 km^2 . It experiences tropical climate conditions with summer temperatures ranging from 38° to 45°C and winter temperatures ranging from 15° to 28°C .

The soil distribution in the region mainly falls under the clay soil's (black cotton soils) category with a mix of silt. The grounds are very fertile, which produce about two to three harvests in a year. Rice is the major crop in this region. Though there are enough rainfalls in the area, most agriculture depends on groundwater due to the lack of proper rainfall water storage, watershed management practices, and distribution network.

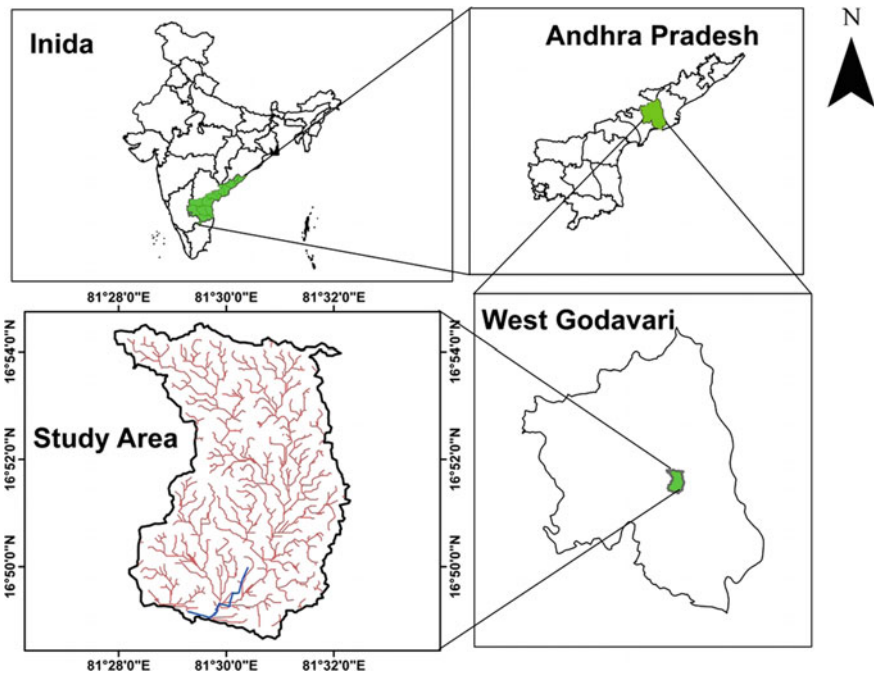


Fig. 1 Location map of study area

Table 1 Details of data used

Type	Details	Source
Toposheets	Nos. 65 H/9 SW and 65 H/5 SE at 1:25,000 scale	Survey of India (SOI)
Satellite data	Landsat 8 band data for the years 2019, 2020 and 2021 at 30 m resolution	USGS EarthExplorer
Rainfall data	Rainfall in mm	Automatic Weather Station at NIT Andhra Pradesh, Tadepalligudem

2.2 Data Collection

Table 1 shows the details of the data used and its sources. Toposheets of no's 65 H/9 SW and 65 H/5 SE, which are of 1:25,000 scale, were purchased from the Survey of India (SOI).

These toposheets are used in delineating watershed boundary as shown in Fig. 1. USGS EarthExplorer, an open-source (<https://earthexplorer.usgs.gov/>), is used to acquire the Landsat 8 satellite data. Downloaded Landsat 8 cloud-free band datasets are covering the study area during November 2019, October 2020, and March 2021 which are used in the study. Rainfall data used in the study are collected from Automatic Weather Station which located at 16⁰50'02.7" north latitude and 81⁰29'09" east longitude covering the study region.

2.3 Methodology

Figure 2 shows the flowchart representation of the methodology followed in this study. Watershed boundary is delineated using the toposheets purchased. The boundary delineated is further used on Landsat 8 band data to clip the datasets to the boundary scale. Landsat 8 datasets are used in the generation of Normalized Difference Vegetation Index (NDVI) and Soil-Adjusted Vegetation Index (SAVI) maps. SAVI is used in the generation of LAI maps; this LAI is further used in the generation of canopy storage capacity (S_{max}). LAI, canopy storage capacity, and rainfall data are used in the interception model to generate spatiotemporal variation maps of canopy rainfall interception.

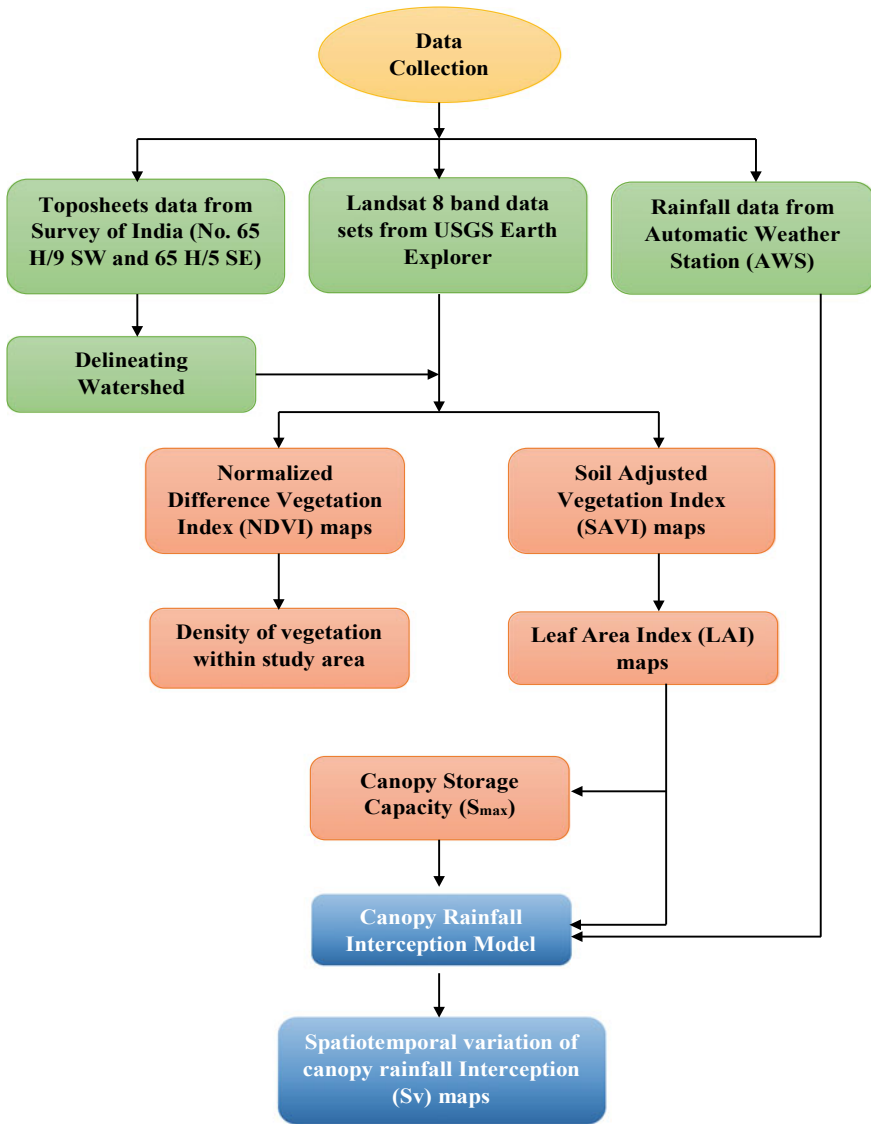


Fig.2 Flow chart of methodology

2.4 Selection of Input parameters

2.5 Normalized Difference Vegetation Index (NDVI)

Normalized Difference Vegetation Index (NDVI) is one of the indexes derived using remote sensing data. It is a dimensionless parameter that ranges from -1 to $+1$. It is used as an indicator to understand the density of vegetation cover. The higher value of NDVI indicates healthy vegetation cover. The NDVI map for Landsat 8 satellite is generated using Eq. (1).

$$\text{NDVI} = \frac{\text{Band 5} - \text{Band 4}}{\text{Band 5} + \text{Band 4}} \quad (1)$$

Band 5 indicated near-infrared (NIR) band, and Band 4 indicated red band.

2.6 Soil-Adjusted Vegetation Index (SAVI)

Soil-Adjusted Vegetation Index (SAVI) is another vegetation index derived using remote sensing data. It is used as a correction to NDVI to minimize the impact of soil brightness in low vegetation cover regions by using the soil brightness correction factor. SAVI is given by Delegido et al. [17], as shown in Eq. (2).

$$\text{SAVI} = \frac{(\text{Band 5} - \text{Band 4})}{(\text{Band 5} + \text{Band 4} + L)} \times (1 + L) \quad (2)$$

Band 5 indicated the near-infrared (NIR) band, Band 4 indicated the red band, and L is the soil brightness correction factor. L is taken as 1 in case of no vegetation, 0.5 in moderate vegetation conditions, and 0 in high dense vegetation scenarios [17]. In this study area, L is taken as 0.5.

2.7 Leaf Area Index (LAI)

Leaf area index (LAI) is used to indicate the rate of vegetation growth in an area. It is defined as the total one-sided leaf area per unit ground surface area [18, 19]. LAI from the METRIC method is given by De Wasseige et al. [20], as shown in Eq. (3).

$$\text{LAI} = -\frac{\ln\left(\frac{0.69 - \text{SAVI}}{0.59}\right)}{0.91} \quad (3)$$

where SAVI is the Soil-Adjusted Vegetation Index.

2.8 Canopy Rainfall Interception Model

The primary factor in estimation interception by vegetation is the canopy storage capacity (S_{\max}). Canopy storage capacity, also known as the maximum interception storage capacity, is given by [21], as shown in Eq. (4).

$$S_{\max} = 0.935 + (0.498 \times \text{LAI}) - (0.00575 \times \text{LAI}^2) \quad (4)$$

where LAI is the leaf area index.

Canopy cumulative interception during a rainfall event is given by Aston [22] which is modified from [23] as shown in Eq. (5).

$$S_v = S_{\max} \times \left[1 - e^{-\eta \frac{P_{\text{cum}}}{S_{\max}}} \right] \quad (5)$$

where S_v represents canopy rainfall interception in mm, P_{cum} shows the value of cumulative precipitation in mm for a rainfall event, and η is the correction factor ($\eta = 0.046 \times \text{LAI}$).

The assumption made by Aston [22] for Eq. (5) is: if cumulative rainfall is equal to zero, then canopy rainfall interception is also zero. But, in the case of cumulative rainfall approaching infinity, then canopy rainfall interception is equal to canopy storage capacity.

3 Results and Discussions

3.1 Spatiotemporal Variation Patterns of NDVI

NDVI maps are generated using Eq. (1). The maps are generated for the years 2019, 2020, and 2021 as shown in Fig. 3. It is observed that the value of NDVI is within the range of -1 to $+1$. The maximum value of NDVI is 0.548, 0.39, and 0.45 in the year 2019, 2020, and 2021, respectively. There is a decrease in NDVI value in the year 2020, because it is crop harvesting and sowing period. The study area contains fertile soil with good agricultural conditions, and it is observed that vegetation coverage is seen at almost 75% (considering three months as the gap between harvesting and sowing for each crop season) of the year. It is noted that the maximum NDVI value ranges from 0.4 to 0.55 in the study area, indicating a good density of vegetation cover in the study area.

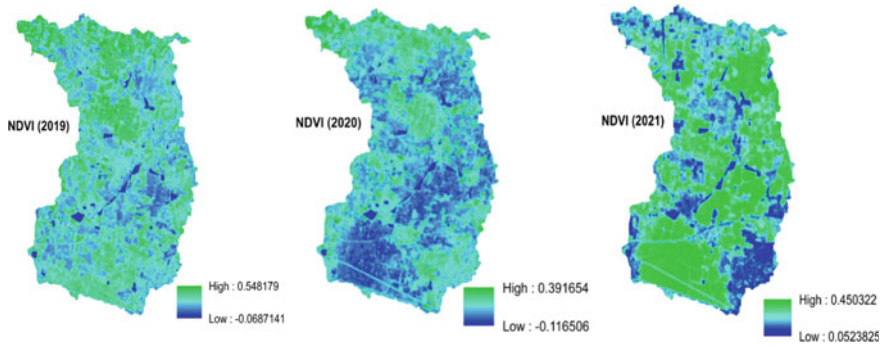


Fig. 3 Spatial patterns of NDVI in study area

3.2 Spatiotemporal Variation Patterns of LAI

LAI maps are generated using Eqs. (3) and (4). LAI maps for the years 2019, 2020 and 2021 are shown in Fig. 4. The LAI indicates the growth rate of vegetation, so the high value indicates a reasonable growth rate. It can be observed that for the year 2019, though the maximum LAI value is 9.55, the area under that category of high LAI value is very low; most of the study area is in the range of -0.325 to 4.612 , so the average LAI is approximately 2.143. For 2020, it can be spotted that most of the study area is under the LAI value of 0.75 or below. But, for 2021, the maximum LAI value of 4.07 is observed in 50% of the study area. The average LAI value decreased from 2.143 in 2019 to 0.75 in 2020, mainly because the data collected for 2020 are in October, during which seasonal crop change occurs. The average value of LAI in 2021 increased to 2.01. LAI values generated can support the study area which has good fertile soil, which can harvest two or three crop seasons in a year.

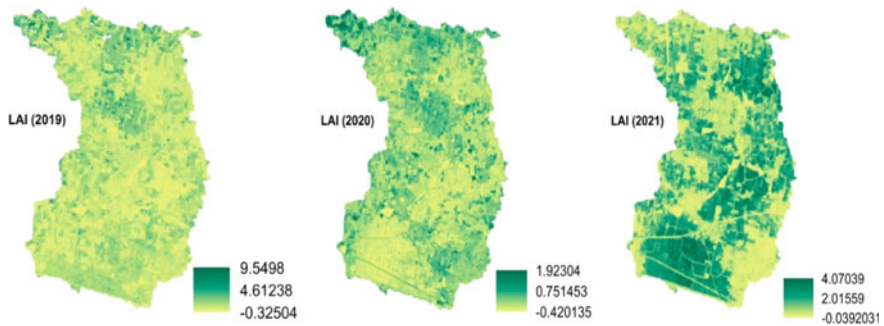


Fig. 4 Spatial patterns of LAI in study area

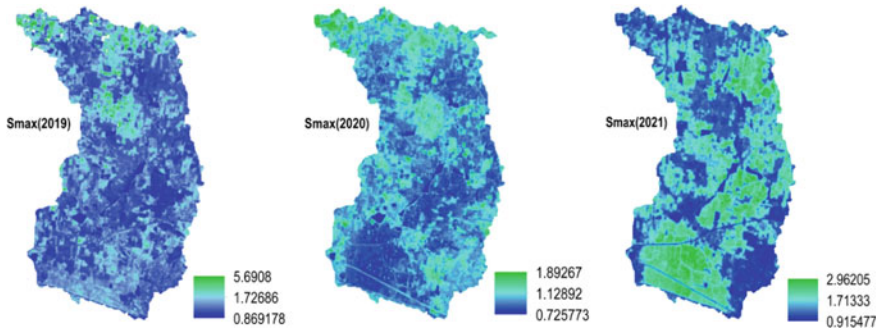


Fig. 5 Spatial patterns of canopy storage capacity (S_{max}) in study area

3.3 *Spatiotemporal Variation Patterns of Canopy Storage Capacity (S_{max})*

Canopy storage capacity (S_{max}) is the maximum quantity of interception that the canopy can store. Canopy storage capacity maps are generated using Eq. (4) of canopy rainfall interception model. Canopy storage capacity maps for the years 2019, 2020, and 2021 are shown in Fig. 5. Similar to the LAI maps, though the maximum canopy storage capacity value was high in 2019, the area covered under that increased value is minimal. So, it is better to consider average values for all the years. The average canopy storage capacity value for 2019, 2020, and 2021 is 1.726, 1.28, and 1.71, respectively. It is a good indicator that interception plays a crucial role in the hydrological cycle. So, interception cannot be neglected in the hydrological studies for this region.

3.4 *Spatiotemporal Variation Patterns of Canopy Rainfall Interception (S_v)*

Canopy rainfall interception (S_v) maps are generated using Eq. (5) of canopy rainfall interception model. The value ranges in the maps indicate the canopy rainfall interception with the unit of mm. One of the components in canopy rainfall interception estimation is cumulative rainfall (mm). The study is conducted for three rainfall events to understand the variation in canopy rainfall interception with changes in precipitation. The rainfall events over the years 2019, 2020 and 2020 are categorized as maximum cumulative rainfall event, moderate cumulative rainfall event, and low cumulative rainfall event. The cumulative rainfall amounts considered in the study are:

- (i) Maximum cumulative rainfall = 165.25 mm
- (ii) Moderate cumulative rainfall = 40 mm
- (iii) Low cumulative rainfall = 15 mm

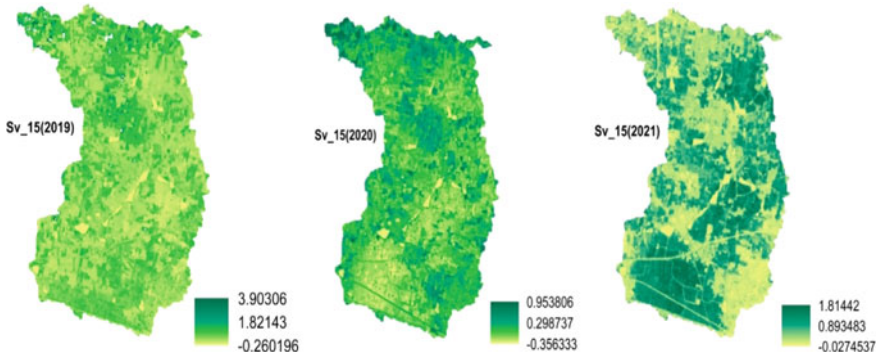


Fig. 6 Spatial patterns of canopy rainfall interception (S_v) for 15 mm rainfall event in study area

The maximum rainfall of 165.25 mm in the study area occurred during the 12th and 13th of October 2020. The maps are generated for each rainfall event. A total of nine maps are developed for different periods and with varying amounts of precipitation.

Canopy rainfall interception (S_v) maps during 15 mm of precipitation for the years 2019, 2020, and 2021 are shown in Fig. 6. From the generated maps, it is observed that a significant portion of the surface area is contributing to interception. The canopy rainfall interception values for 15 mm rainfall event are 1.83, 0.95 and 1.81 mm during 2019, 2020, and 2021, respectively. It indicates that for the 15 mm quantity of rainfall received, on average, 1.53 mm of rainfall received is lost in the form of interception.

Canopy rainfall interception (S_v) maps during 40 mm of precipitation for the years 2019, 2020, and 2021 are shown in Fig. 7. From the generated maps, it is observed that a significant portion of the surface area is contributing to interception. The canopy rainfall interception values for 40 mm rainfall events are 2.26, 1.6 and 2.72 mm during 2019, 2020, and 2021, respectively. It indicates that for the 40 mm quantity of rainfall received, on average, 2.2 mm of rainfall received is lost in the form of interception.

Canopy rainfall interception (S_v) maps during 165 mm of precipitation for the years 2019, 2020, and 2021 are shown in Fig. 8. From the generated maps, it is observed that the maps of the canopy rainfall interception values for 165 mm rainfall events are 5.69, 1.89 and 2.96 mm during 2019, 2020, and 2021, respectively. It indicates that for the 165 mm quantity of rainfall received, on average, 3.5 mm of rainfall is lost in the form of interception.

If you observe Figs. 5 and 8, the maximum values for both canopy storage capacity (S_{max}) and canopy rainfall interception (S_v) for 165 mm rainfall events are the same proving the assumption made by [22]. In the study area, it is recognized that the maximum storage capacity of vegetation is reached when the cumulative rainfall is above 40 mm and under 165 mm.

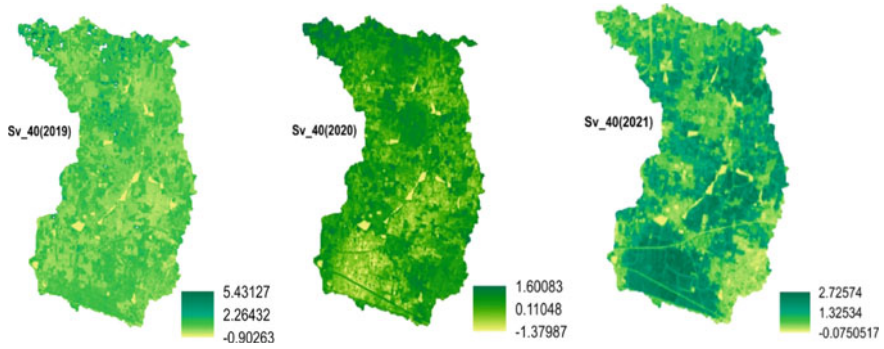


Fig. 7 Spatial patterns of canopy rainfall interception (S_v) for 40 mm rainfall event in study area

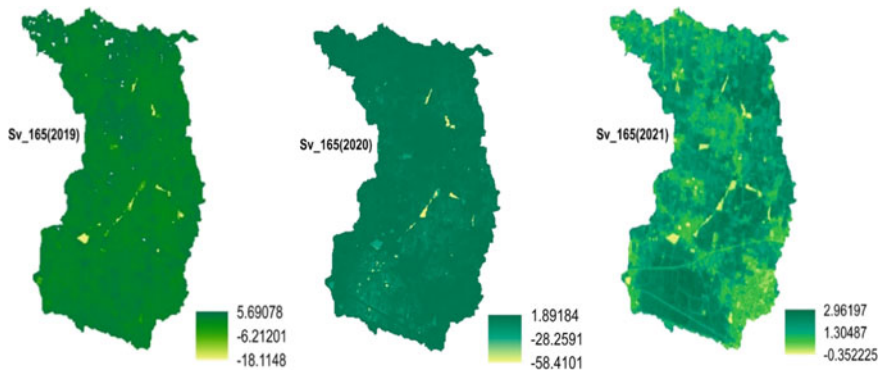


Fig. 8 Spatial patterns of canopy rainfall interception (S_v) for 165 mm rainfall event in study area

4 Conclusions

The canopy rainfall interception is being effectively assessed with the combination of remote sensing and interception model. The outcomes offer insight into the variation of canopy rainfall interception at both spatial and temporal scales within the study area. Depending on the rainfall event, nearly 1–5.7 mm of rainfall received is being lost due to the interception by vegetation over the years 2019–2021; it is apparent that a significant quantity of precipitation is lost in the form of interception in areas covered with vegetation and crops. Hence, it can be acknowledged that interception plays a significant role in the hydrological processes even at a regional scale. The present methodology applies to micro to medium level watersheds in different geographical regions. The interception results obtained from this study will be helpful for rainfall and runoff studies within the study area.

Acknowledgements This research is funded by the Department of Science and Technology-Science and Engineering Research Board (DST-SERB) sponsored project bearing the sanction

number EEQ/2019/000463 undertaken in the Department of the Civil Engineering, NIT Andhra Pradesh, titled Monitoring and Analysis Nonpoint Source Pollutants in Agricultural Watershed using Soil Water Assessment Tool (SWAT) under Principal Investigation of Dr T. Reshma Assistant Professor.

References

1. Murakami S (2006) A proposal for a new forest canopy interception mechanism: splash droplet evaporation. *J Hydrol* 319:72–82. <https://doi.org/10.1016/j.jhydrol.2005.07.002>
2. Tsiko CT, Makurira H, Gerrits AMJ, Savenije HHG (2012) Measuring forest floor and canopy interception in a savannah ecosystem. *Phys Chem Earth Parts ABC* 47–48:122–127. <https://doi.org/10.1016/j.pce.2011.06.009>
3. Zhang Y, Li XY, Li W, et al (2017) Modeling rainfall interception loss by two xerophytic shrubs in the Loess Plateau
4. Wu J, Liu L, Sun C et al (2019) Estimating rainfall interception of vegetation canopy from MODIS imageries in Southern China. *Remote Sens* 11:1–19. <https://doi.org/10.3390/rs11212468>
5. Dunkerley D (2000) Measuring interception loss and canopy storage in dryland vegetation: a brief review and evaluation of available research strategies. *Hydrol Process* 14:669–678. [https://doi.org/10.1002/\(SICI\)1099-1085\(200003\)14:4%3c669::AID-HYP965%3e3.0.CO;2-I](https://doi.org/10.1002/(SICI)1099-1085(200003)14:4%3c669::AID-HYP965%3e3.0.CO;2-I)
6. Carlyle-Moses DE, Laureano JSF, Price AG (2004) Throughfall and throughfall spatial variability in Madrean oak forest communities of northeastern Mexico. *J Hydrol* 297:124–135. <https://doi.org/10.1016/j.jhydrol.2004.04.007>
7. Peng H, Zhao C, Shen W et al (2009) Modeling canopy interception of Piceacrassifolia forest in Qilian Mountains using quickbird satellite data. *Int Geosci Remote Sens Symp IGARSS* 4:370–373. <https://doi.org/10.1109/IGARSS.2009.5417390>
8. Cui Y, Zhao P, Yan B et al (2017) Developing the remote sensing-gash analytical model for estimating vegetation rainfall interception at very high resolution: a case study in the Heihe River Basin. *Remote Sens* 9:1–12. <https://doi.org/10.3390/rs9070661>
9. Rutter AJ, Morton AJ, Robins PC (1975) A predictive model of rainfall interception in forests. II. Generalization of the model and comparison with observations in some coniferous and hardwood stands. *J Appl Ecol* 12:367. <https://doi.org/10.2307/2401739>
10. Rutter AJ, Morton AJ (1977) A predictive model of rainfall interception in forests. III. sensitivity of the model to stand parameters and meteorological variables. *J Appl Ecol* 14:567. <https://doi.org/10.2307/2402568>
11. Gash JHC, Lloyd CR, Lachaud G (1995) Estimating sparse forest rainfall interception with an analytical model. *J Hydrol* 170:79–86. [https://doi.org/10.1016/0022-1694\(95\)02697-N](https://doi.org/10.1016/0022-1694(95)02697-N)
12. Dunkerley DL (2008) Intra-storm evaporation as a component of canopy interception loss in dryland shrubs: observations from Fowlers Gap, Australia. *Hydrol Process* 22:1985–1995. <https://doi.org/10.1002/hyp>
13. Jr DFL, Frost EE (2003) A review and evaluation of stemflow literature in the hydrologic and biogeochemical cycles of forested and agricultural ecosystems. *J Hydrol* 274:1–29
14. Wang XP, Zhang YF, Wang ZN et al (2013) Influence of shrub canopy morphology and rainfall characteristics on stemflow within a revegetated sand dune in the Tengger Desert, NW China. *Hydrol Process* 27:1501–1509. <https://doi.org/10.1002/hyp.9767>
15. de Jong SM, Jetten VG (2007) Estimating spatial patterns of rainfall interception from remotely sensed vegetation indices and spectral mixture analysis. *Int J Geogr Inf Sci* 21:529–545. <https://doi.org/10.1080/13658810601064884>
16. Delegido J, Fernandez G, Gandia S, Moreno J (2008) Retrieval of chlorophyll content and LAI of crops using hyperspectral techniques: application to PROBA/CHRIS data. *Int J Remote Sens* 29:7107–7127. <https://doi.org/10.1080/01431160802238401>

17. Huete AR (1988) A soil-adjusted vegetation index (SAVI). *Remote Sens Environ* 25:295–309
18. Bréda NJJ (2003) Ground-based measurements of leaf area index: a review of methods, instruments and current controversies. *J Exp Bot* 54:2403–2417. <https://doi.org/10.1093/jxb/erg263>
19. De Wasseige C, Bastin D, Defourny P (2003) Seasonal variation of tropical forest LAI based on field measurements in Central African Republic. *Agric For Meteorol* 119:181–194. [https://doi.org/10.1016/S0168-1923\(03\)00138-2](https://doi.org/10.1016/S0168-1923(03)00138-2)
20. Allen RG, Tasumi M, Morse A et al (2007) Satellite-based energy balance for mapping evapotranspiration with internalized calibration (METRIC)—applications. *J Irrig Drain Eng* 133:395–406. [https://doi.org/10.1061/\(asce\)0733-9437\(2007\)133:4\(395\)](https://doi.org/10.1061/(asce)0733-9437(2007)133:4(395))
21. De Roo API, Wesseling CG, Ritsema CJ (1996) Lisem: a single-event physically based hydrological and soil erosion model for drainage basins. I: theory, input and output. *Hydrol Process* 10:1107–1117. [https://doi.org/10.1002/\(sici\)1099-1085\(199608\)10:8%3c1107::aid-hyp415%3e3.0.co;2-4](https://doi.org/10.1002/(sici)1099-1085(199608)10:8%3c1107::aid-hyp415%3e3.0.co;2-4)
22. Aston AR (1979) Rainfall interception by eight small trees. *J Hydrol* 42:383–396. [https://doi.org/10.1016/0022-1694\(79\)90057-X](https://doi.org/10.1016/0022-1694(79)90057-X)
23. Merriam RA (1960) A note on the interception loss equation. *J Geophys Res* 65:3850–3851. <https://doi.org/10.1029/jz065i011p03850>